# THALIDOMIDE-INDUCED TERATOGENESIS IN GRAY SHORT-TAILED OPOSSUMS (*MONODELPHIS DOMESTICA*)

BY

DANIEL SORENSEN

THESIS

Submitted in partial fulfillment of the requirements
for the degree of Master of Science in Biology
with a concentration in Ecology, Ethology, and Evolution
in the Graduate College of the
University of Illinois at Urbana-Champaign, 2015

Urbana, Illinois

Master's Committee:

Assistant Professor Karen Sears, Director of Research
Professor Lisa Stubbs
Assistant Professor Princess Imoukhuede

ABSTRACT

From 1957 to 1962, Thalidomide was prescribed to pregnant women as an antiemetic and was later discovered to cause serious birth defects. Thalidomide is currently being prescribed to treat erythema nodosum leprosum and multiple melanoma, and is being considered for other anti-angiogenic applications. This is of concern, as the mechanisms by which thalidomide disrupts development remain largely unknown. This lack of knowledge is largely due to the absence of an appropriate model mammalian system. Traditional mammal models, such as rats and mice, are resistant to the teratogenic properties of thalidomide. We propose to develop the gray short-tailed opossum (*Monodelphis domestica*) as a novel mammalian to study thalidomide teratogenesis. In *M. domestica* we have successfully recreated most morphological defects found in human thalidomide victims. Through RNA sequencing, we have also identified two gene that may play a significant role in the mechanism of thalidomide induced birth defects.

# TABLE OF CONTENTS

INTRODUCTION……1
METHODS…… 5
RESULTS…… 7
DISCUSSION……11
REFERENCES……13
FIGURES AND TABLES…… 16

# INTRODUCTION

Thalidomide was originally marketed in 1957 as a non-barbiturate sedative. The drug's mild side effects on the patient made it incredibly popular in the treatment of morning sickness. In 1959 thalidomide was found to cause a wide spectrum of very serious birth defects. The drug was completely removed from the market by 1962. Thalidomide is estimated to be responsible for affecting birth defects in over 10,000 children in Germany alone (Dove, 2011). As thalidomide was sold in a large number of nations other than the United States, the total number of victims cannot be accurately estimated. The release of thalidomide into the market is widely considered to be the worst medical regulatory failure in history. Despite its sordid history, thalidomide reemerged on the market in 1965 as a treatment for erythema nodosum leprosum. In 1998 thalidomide also began to be used to help treat multiple myeloma, and other anti-angiogenic applications of the drug are being developed (Calabrese & Fleischer, 2000). Unfortunately, thalidomide's revival has been accompanied by a second generation of children with thalidomide-induced birth defects. In fact, children continue to be born with thalidomide-induced deformities; with at least 100 cases documented in Brazil between 2005 and 2010 (Crawford, 2013).

Despite its long and devastating history, the teratogenic mechanisms of thalidomide remain poorly understood. This lack of knowledge and the early misuse of the drug are primarily due to a lack of an appropriate mammalian model study system for the impact of thalidomide on mammalian development. Traditional mammal models, such as rats and mice, are resistant to the teratogenic properties of thalidomide. Though susceptible, studies of rabbit and other primates are hampered by the number of affected embryos that can be obtained (Vargesson, 2009). Until now, this has left two other types of study systems: non-mammalian vertebrates and human cell cultures. Much of what is known about the mechanisms through which thalidomide causes limb deformations comes from research in non-mammalian vertebrates, such as chickens and zebrafish. Though fully vulnerable to thalidomide defects, wings and fins develop differently enough to severely limit what can be learned about the limb defect. Furthermore the window of thalidomide sensitivity is notably later in chickens than in mammals. Humans are susceptible to thalidomide induced limb defects from the time of the initial formation of the limb bud. In contrast, thalidomide susceptibility in chicken limbs does not begin until well after both limb buds are formed and the forelimb has enlarged significantly (Knobloch, Shaughnessy, & Rüther, 2007). Human cell cultures, most commonly human umbilical vein endothelial cells (HUVECS), are not subject to these cross taxa limitations. They have also been very useful in understanding the thalidomide's effect on a cellular level. However they lack the developmental and

cross-tissue context which limits what can be learned about the mechanisms by which thalidomide generates limb deformities.

We propose to develop the gray short-tailed opossum (*Monodelphis domestica*) as a novel mammalian to study thalidomide teratogenesis. Unlike rodents, we show that opossums are vulnerable to thalidomide-induced limb deformities. Opossums are the first fully susceptible mammal for which affected embryos can be obtained in large numbers. Furthermore, *M. domestica* is a well-established study system for limb development and has a fully sequenced and well-annotated genome (Mikkelsen et al., 2007). *M. domestica* also displays a unique mode of limb development that makes it well suited for studying limb deformities. Specifically, *M. domestica* forelimbs grow at twice the rate of their hind limbs, which provides two temporal opportunities to study thalidomide-induced limb deformities (Doroba & Sears, 2010; Keyte & Smith, 2008). Here we show that *M. domestica* is an effective model organism to investigate the teratogenic impacts of thalidomide and, based on our research in *M. domestica*, propose a novel mechanism for thalidomide-induced digit reduction in mammals.

**Thalidomide Effects -** Thalidomide was originally marketed as a non-barbiturate sedative. The adult side effects are mild and include: constipation, edema, hypocalcaemia, shortness of breath and peripheral neuropathy (Sekeres & List, 2006; Tseng, Pak, Washenik, Pomeranz, & Shupack, 1996). Thalidomide is currently only marketed for anti-angiogenic applications such as erythema nodosum leprosum and multiple myeloma.

However it is thalidomide's teratogenic effects that have proved most catastrophic. Thalidomide birth defects are characterized by a very specific window of sensitivity. In humans, thalidomide birth defects have only been observed when the drug is administered between 20 and 36 days post-fertilization. The most potent defects occur between 27-33 days post-fertilization (Lenz & Knapp, 1962). Treatment prior to day 20 has been shown to induce miscarriage in humans and is hypothesized to be caused by heat malformations (Miller & Strömland, 1999; Vargesson, 2009). Thalidomide treatment after the period of sensitivity has only been shown to increase the risk of autism and interfere with the angiogenesis of parts of the brain (Vargesson, 2013). The vast majority of thalidomide defects occur during the window of sensitivity.

The most recognizable defects caused by thalidomide are those impacting the limbs. The most common of these limb deformities is phocomelia of the upper limb. Phocomelia is the severe truncation of the limb, usually the more proximal elements, with fully formed distal elements such as the hand and digits. Other limb deformities have also been noted such as radial dysplasia, triphalangeal thumb, and

amelia(Miller & Strömland, 1999). Lower limb deformities are less common and usually only occur when upper limb deformities are present (Lenz & Knapp, 1962; Vargesson, 2013).

Non-limb thalidomide defects are diverse and variable. The most common of these are heart defects. These heart defects may be the cause of much of the thalidomide-induced embryonic death prior to 20 days in humans. Liver hypoplasia, irregular vertebral spacing, shoulder and hip deformities are also used to diagnose thalidomide teratogenesis. Deafness and blindness have also been linked to a wide spectrum of thalidomide ear and eye defects. Many other less common thalidomide deformities occurring during the window of sensitivity have also been documented (Smithells & Newman, 1992; Vargesson, 2013).

**Dosage sensitivity -** As thalidomide is water insoluble, it is given to humans in oral tablets. In other mammals, it is dissolved in dimethyl sulfoxide (DMSO) and delivered via gavage feeding or intraperitoneal injection. Thalidomide's historical dosage varied widely, from a 25mg-400mg daily, though it could have been taken in greater amounts as it was available without a prescription in Japan and West Germany. Modern therapeutic doses range from as little as 50mg for multiple myeloma to as much as 400mg for erythema nodosum leprosum. Thalidomide is an extremely potent teratogen. A single 50mg dose of the drug was sufficient to cause miscarriage in humans (Lenz & Knapp, 1962) and the minimum teratogenic dosage has not been determined *in utero*. 50µg/mL has been demonstrated to be the minimal concentration to inhibit cell migration in endothelial cell culture (Tamilarasan et al., 2006).

**Primary Binding -** Thalidomide has two isomeric forms, R (+) and S (-). The S (-) is believed to be an effective sedative while the R (+) is believed to be responsible for the teratogenic effects. An enantiomeric stable version of the S(-) form has been demonstrated to be responsible for thalidomide's anti-inflammatory and tumor suppressing activities (Jacques, Czarnik, Judge, Van der Ploeg, & DeWitt, 2015). However, the teratogenic properties of this stabilized drug remain untested. Thalidomide is also known to form at least 20 metabolites, many of which can exert their own immunomodulatory, anti-inflammatory, or anti-angiogenic function (Ando, Fuse, & Figg, 2002; Tseng et al., 1996). The variety of biologically active products make thalidomide a very difficult drug to study using biochemical approaches.

Only recently has the primary binding target of Thalidomide been identified as Cereblon (*CRBN*)(Ito et al., 2010). *CRBN* forms an E3 ubiquitin ligase with Damaged DNA Binding Protein 1 (DDB1) and Cullin 4A (Cul4A). Zebrafish *CRBN* mutants that reduce thalidomide binding affinity are not susceptible to thalidomide-induced limb defects. Human *CRBN* overexpression has also been

demonstrated to be sufficient to rescue thalidomide-induced birth defects in these in chickens (Fischer et al., 2014; Ito, Ando, & Handa, 2011; Ito et al., 2010). However, research in human cell lines has shown that natural thalidomide resistance is not imparted by mutations in either in either CRBN or DDB1 (Thakurta et al., 2014). *CRBN* is also very well conserved across taxa and is ubiquitously expressed in opossum development(Ito et al., 2010). These lines of evidence suggest that the CRNB complex is necessary but not sufficient to cause thalidomide-induced teratogenesis and is likely not the source of the species or tissue specific nature of the drug. Multiple non-exclusive mechanisms have been used to explain the downstream effects of thalidomide, such as angiogenic antagonization, free radical production, and fibroblast growth factor patterning disruptions (Ito et al., 2011; Knobloch & Rüther, 2008; Vargesson, 2013).

**Anti-Angiogenic Properties -** Thalidomide's best studied function is as a powerful anti-angiogenic. By inhibiting beta fibroblast growth factor (*bFGF*) and vascular endothelial growth factor *(VEGF)*, thalidomide is able to inhibit blood vessel maturation or angiogenesis in all studied taxa (Kenyon, Browne, & D'amato, 1997). Thalidomide has been shown to reduce microvessel density and is being explored in a variety of therapeutic applications, such as the treatment of hereditary hemorrhagic telangiesctasia (Du et al., 2004; Lebrin et al., 2010). Though the connection between the primary *CRBN* binding and the anti-angiogenic effects remains unclear, much is still known about thalidomide phenotype. Key regulators of angiogenesis such as *VEGF, IL-8, bFGF8* and members of the hedgehog signaling pathways have been shown to be significantly depleted with thalidomide treatment. Thalidomide does not appear to cause any major changes in endothelial cell proliferation but does significantly alter endothelial cellular migration. (Komorowski et al., 2006; Tamilarasan et al., 2006)

However, almost all of these anti-angiogenic experiments have been performed in human culture, mouse, or zebrafish models. This has severely limited their ability to explain the links between anti-angiogenic properties and limb deformities in humans. In one of the few studies that was able to bridge this gap in knowledge, Therapontos et al. demonstrated that CSP49, an anti-angiogenic analog of thalidomide, is able to cause vascular defects prior to changes in *FGF8* expression, which is believed to be involved in the limb patterning defects (Therapontos, Erskine, Gardner, Figg, & Vargesson, 2009). However, this is contrasted by Ito et al which found that zebrafish fin patterning is disrupted prior to vascularization of the limb. The applicability of both of these studies to humans is hampered by lack of an appropriate mammalian model for thalidomide-induced birth defects.

**Other Teratogenic Outcomes -** Other non-mutually exclusive theories have been used to explain thalidomide's teratogenic outcomes, such as the excessive accumulation of reactive oxygen species

(ROS). Experiments using spin trapping agents have demonstrated that an overabundance of ROS are required for thalidomide to inhibit blood vessel formation (Parman, Wiley, & Wells, 1999). Furthermore, there is three times more DNA oxidation in treated rabbits than treated mice (which suggest the role of ROS in the species specific nature of thalidomide (Knobloch & Rüther, 2008).

In this study we tested the susceptibility of *M. domestica* development to disruption by exposure to thalidomide. To do this we administered thalidomide to pregnant females, and observed the resulting impact on gross anatomy, cellular processes including death and proliferation, vascularization, and patterns of gene expression. To do this we administered thalidomide to pregnant females, and observed the resulting impact on gross anatomy, cellular processes including death and proliferation, vascularization, and patterns of gene expression. We hypothesize of the model research animals that embryos can easily be obtained, *M. domestica* best represents the human thalidomide phenotype.

## METHODS

**Tissue Collection -** We maintain a breeding colony with approximately 75 *M. domestica* with detailed pedigrees, at University of Illinois at Urbana Champaign (UIUC). All procedures are in accordance with the UIUC IACUC. *M. domestica* are bred using standard breeding and embryo collection protocols (Keyte & Smith, 2008). Mating cages with a single male and female animal are paired and infrared video recording used to observe and establish exact mating times. Doses of 500-1000µg of thalidomide were dissolved in phosphate buffered saline (PBS) with 1% carboxymethyl cellulose and 1% dimethyl sulfoxide (DMSO). This solution or a control solution of similar composition but without thalidomide was administered at stage 26 (10.75 hours after mating). Opossums were euthanized via carbon dioxide inhalation at time points thereafter, and embryos staged according to (Smith, 2002).

**Skeletal and Vascular Morphology -** For the morphology assessments, pregnant opossums were euthanized 3 days post treatment with carbon dioxide to effect followed by cervical dislocation. Embryos were immediately photographed then fixed in 4% paraformaldehyde in PBS before being dehydrated and stored in methanol (MeOH). A single fore- and hindlimb were removed from the embryo. The remaining embryo was cleared and stained to visualize the cartilage of the developing skeleton using alcian blue (Hanken & Wassersug, 1981).

Dissected limbs were rehydrated into PBS and washed for 5 hours in Tris-buffered saline (TBS) with 1% Triton X-100. To label vasculature, the limbs were then incubated for 48 hours in fetal bovine serum with 0.05% dimethyl sulfoxide with Isolectin GS-IB4 from *Griffonia simplicifolia*, Alexa Fluor® 488

Conjugate antibody (Life Technologies). Limbs were counterstained using 40 6-diamidino-2-phenylindole (DAPI) (Vectashield Mounting Media with DAPI). Vascularization was quantified by counts of distinct branch counts of blood vessels over five 1.25mm$^2$ regions of each labeled using ImageJ. Significance was evaluated using a Wilcoxon Rank Sums Test (P threshold=0.05).

**Cell Death and Proliferation -** For the cell death and proliferation experiments, 12 hours after treatment with either thalidomide or DMSO control [at late stage 27 (11.25 days post mating)] pregnant opossums were euthanized as described above. Embryos were fixed in 4% paraformaldehyde in PBS before being stored in MeOH. Embryos were then rehydrated into PBS and immersed in 30% sucrose in PBS for 12 hours. Tissues were equilibrated in Optimal Cutting Temperature (OCT) compound embedding media (Tissue-Tek) for 2 hours then frozen. 10μm sections of the forelimb in the frontal plane were taken using a cryotome.

Apoptotic cells were visualized using the ApopTag Fluorescein Direct In Situ Apoptosis Detection Kit (S7100, Millipore). Three mid limb sections were per embryo from three DMSO treated control embryos and three thalidomide treated embryos. Apoptosis was quantified via cell counts of florescent cells per overall number of cells in the limb bud. Three sections were sampled per limb and florescence counts were repeated three times. Significance was evaluated using Mann-Whitney *U* Test on the proportion of total limb cells fluorescing (P value threshold =.05)

Proliferating cells were detected using an antibody against phospho-histone H3 (Ser 10; Cell Signaling Technology, 9701). Three mid limb sections were sampled from three DMSO control treated embryos and a total of eight mid limb sections were sample from four different thalidomide treated embryos. The primary antibody was applied for 24 hours with 1% heat inactivated goat serum and 0.1% Triton X-100 in PBS for 12 hours at 4°C. The sections were then washed and incubated with fluorescent Alexa Fluor 488 goat anti-rabbit antibody (Invitrogen A31627). Sections were imaged and quantified in the same manner as the apoptotic cells. Nuclei were also counterstained using 40 6-diamidino-2-phenylindole (DAPI) (Vectashield Mounting Media with DAPI).

**RNA Sequencing -** Pregnant opossums were euthanized 30 minutes after treatment at stage 26 (10.77 hours post mating). Two control and three Thalidomide-treated whole embryos were dissected into RNAlater (Ambion) and total RNA extracted using the E.Z.N.A Total RNA Kit 1 (Omega). Single-ended RNASeq libraries were made using TruSeq RNA Sample Preparation Kit Version 2 (Illumina). Libraries were sequenced by the University Of Illinois Roy G. Carver Biotechnology Center using an Illumina HiSeq 2500.

The sequence output was processed by removing adapter ends and reads with a Phred score below 33 with Trimmomatic Version 0.33 (Bolger, Lohse, & Usadel, 2014). The remaining reads were aligned to the *M. domestica* reference genome using STAR 2.4.0 (Dobin et al., 2013). The monDom5 assembly and annotation files stored on Ensembl were used (Mikkelsen et al., 2007). EdgeR v3.8.6 was used to identify genes that were differentially expressed due to thalidomide treatment (*P* value threshold = 0.01). Gene expression values were normalized as log transformed counts per million mapped reads (Robinson, McCarthy, & Smyth, 2010). GO term analysis was performed using v6.7 David function annotation tool separately for up and down regulated genes (Huang, Sherman, & Lempicki, 2008).

## RESULTS

Three major phenotypes are present among the 57 thalidomide-treated embryos that are generated by this study. First, the external morphology of 28% (N=16) of the embryos appears normal. They are full size, have normal proportions, and do not display any visible deformities. Second, 60% (N = 34) of embryos display a phenotype that appears mildly affected by thalidomide. These embryos are externally normal with exception of the presence of vascular deformities. Third, 12% (N = 7) of embryos exhibit a severely affected phenotype that is highly variable in external morphology.

The mildly deformed embryos occur in all treated litters (Figure 1). These embryos are indistinguishable from control embryos in terms of overall size and limb patterning. Heartbeats can be visualized upon removal from the mother. A common defect across these embryos is severe internal hemorrhaging, possibly hemangioma(Delahunt & Lassen, 1964). All mildly deformed embryos contain at least one area where large amounts of blood have pooled. These areas are located in the limb and areas surrounding the base of the forelimb, brain, or abdominopelvic cavity. The placement of these hemorrhages are most commonly asymmetrical with the exception the hindlimb which tends to hemorrhage symmetrically. The hindlimb is more commonly hemorrhaged than the forelimb, and the midbrain is the most commonly affected portion of the head. In four of the embryos the amniotic sac was constricted around the embryo just anterior to the hindlimb. These four embryos did not display any signs of morphological deformation or size reduction associated with amniotic band syndrome.

Each of the severely deformed embryos are distinct in morphology. The overall size of these embryos is significantly smaller than normal, and is roughly half the size of unaffected or mildly affected littermates. All but one of these embryos has no pigmentation in the eye. No significant change is

observable in limb vascularization of the zeugopod or autopod between the untreated, mildly affected, and severely affected embryos.

Embryo 1684-1 is the least deformed out of the severely deformed embryos (Figure 2a). Instead of a normal single amniotic sac, the amniotic sac has split into two chambers: one surrounding the embryo and one connecting to the chorionic plate. The vascular network around the heart is largely hemorrhaged. The heart itself is a small mass of improperly organized tissue beneath a single membrane, where it should be fully enclosed in the thoracic cavity by this point in development. While the cranial medial portion of the face appears to be normal above the jaw, there is no apparent mouth opening and the lateral portions of the cranium are missing or remarkably reduced in size. The length of the limb is severely stunted but there are no signs of the phocomelia characteristic of thalidomide. The hindlimb appears to be normal and the only notable change to the forelimb is a symmetrical loss of the first and fifth digit which results in a narrowed autopod.

Embryo 699-1 is also one of the milder of the severely deformed embryos (Figure 2B). Like 1684-1 it has a dual chambered amniotic sac and a large hemorrhage on the ventral surface surrounding the heart. The vascular networks appear immature with none of the early establishment of the major blood vessels. The medial rostral portion of the face is heavily deformed. The medial portion of the mandibular process is severely reduced and the medial nasal process is completely absent. The cranial portion of the head also appears to be reduced in size. The cleared and stained specimens show the limbs are normally patterned despite the overall size reduction. Like embryo 1684-1, this embryo appears to have been viable at least until the point of dissection as demonstrated by the reduction in interdigital tissue and protruding tongue characteristic of stage 33 opossums.

The remaining severely deformed embryos were not clearly alive at the time of dissection as they maintain none of the characteristics of stage 33 opossums and did not have blood flow to the whole embryo. Embryo 613-10 appears to have some blood flow though there are no major arteries (Figure 2c). The entire rostral portion of the cranium is greatly reduced. The entire section of the embryo posterior to the forelimb is reduced in size more than the anterior of the animal. The digits of the forelimbs have failed to differentiate and protrude from the embryo at abnormal and asymmetrical angles.

Embryos 627-1 and 627-2 display similar defects (Figure 2d). Though the faces got damaged during dissection, a significantly reduced mandibular process is still identifiable. Neither embryo contains blood in a visible vascular network. Both hindlimbs are reduced in size and at an immature bud

stage. One hindlimb from embryo 627-1 is severely narrowed. The forelimb development of both appears to be normal.

The forelimbs of embryo 1684-2 are normal in their medial-lateral patterning (Figure 2e). They are, however, missing a single digit leaving the remaining digits in a symmetrical arrangement. The vascular network is incomplete and disorganized. Damage to the head has made cranial identification impossible.

The most disfigured of the embryos is 1684-3 (Figure 2f). It is the smallest embryo collected and is less than a third of the length of the healthy embryos. There are only very small patches of blood-filled vasculature. The limbs are asymmetrical. The left limb resembles an enlarged version of the limb bud of a normal stage 28 opossum. The right limb is severely truncated and reduced in both width and length. Much of the cranial morphology is unidentifiable due to gross deformity but the rostral section of the head appears to be absent or much reduced.

**Vascular Morphology -** No significant changes in vascular morphology has been observed between untreated versus mildly affected embryos (P=0.0638) and untreated versus severely affected embryos (P=0.8895). Even the limbs of the severely affected embryos appear to have similar level of vascular density. However major arteries, such the common carotid and brachial arteries are absent in the severely deformed embryos which suggests that there is some disruption of vascular morphology.

**Cell Death Proliferation/Death -** The sections of the limb were taken during the enlargement of the early limb bud. There was no significant change in the overall number of apoptotic cells (P=0.857) or change in the location of cell death. There was also no change in the overall amount of proliferation in the limb bud (P=0.889). The control sample displayed an even distribution of proliferating cells though out the entire limb. However the thalidomide treated limbs had minimal proliferation in the center of limb (Figure 3). Instead almost all proliferation was localized to the peripheral margins of the bud. There was no apparent distinction in proliferation between the distal, anterior or posterior margins of the limb.

**Gene Expression Changes -** RNAseq analysis identified 1515 significantly upregulated genes and 1854 significantly down regulated genes from stage 26 Thalidomide treatment. It is worth noting that several genes hypothesized to play significant rolls in thalidomide teratogenesis such *as FGF2, FGF8, FGF10, Gsk3β and Sall4* expression are not significantly differentially expressed in these thalidomide treated embryos (Ito et al., 2010; Knobloch & Rüther, 2008; Vargesson, 2013). This does not necessarily mean that these genes do not play a role in thalidomide teratogenesis but suggests that they do not do so during this specific developmental time window. The angiogenesis GO term is significant at similar

levels in both the up- and down- regulated subclasses. The classes of genes that were most strongly upregulated were involved in neuron differentiation and embryonic morphogenesis (Table 1).

Thalidomide syndrome is very similar to the *TBX5* defect, Holt-Oram Syndrome, and the two are often misdiagnosed for each other (Kohlhase et al., 2003). Interestingly, *TBX4* and *TBX5*, which are involved with hind versus fore- limb differentiation, respectively, are both significantly upregulated in treated opossums (Table 2). This is in contrast with other studies that observed a reduction in *TBX5* in Thalidomide-treated HH stage 23/24 chickens (Knobloch & Rüther, 2008).

Both *MEIS1* and *MEIS2* are also significantly upregulated in thalidomide treated limbs. These genes are essential for establishing the proximal boundary of the limb (Mercader et al., 1999). Additionally *MEIS1* mutations display a hemorrhagic phenotype and liver hypoplasia similar to phenotypes that result from thalidomide treatment (Azcoitia, Aracil, Martínez-A, & Torres, 2005; Gershbein, 1965).

More general cell processes such as lipid biosynthesis, steroid metabolism, and transmembrane transport were significantly downregulated upon thalidomide exposure (Table 3). Nine of downregulated genes were represented in the neuropathy GO term. This is interesting as neuropathy is one of the more common side effects of prolonged thalidomide treatment in adults(Efstathiou et al., 2007). TIE-2/TEK, an angiopoietin receptor, was found to be essential for vascular network formation and was significantly downregulated in thalidomide treated limbs (logFC=-0.769). *TIE-2* mutant mice display embryonic vascular and patterning deformities which resemble those of thalidomide-treated opossums (Sato et al., 1995). *TGFBR2* expression was also significantly downregulated in thalidomide exposed embryos (logFC=-.719). Similar to the phenotypes generated by thalidomide exposure, TGFBR2 deficiency can lead to cardiovascular, craniofacial, neurocognitive and skeletal developmental abnormalities (Loeys et al., 2005).

The Apolipoprotein family of genes was found to be significantly downregulated. Not only is this gene family significant in hind versus forelimb patterning but it also has been shown to play a major role in angiogenesis and hindlimb ischemia (Theurl et al., 2015). Another gene that is downregulated in thalidomide treated embryos is *Alx4. Alx4* is known to have significant roles in the morphological patterning of the limb and functions to pattern the anterior-posterior axis of the limb and ZPA restriction (Qu et al., 1997).

## DISCUSSION

Embryonic *M. domestica* that have been exposed to thalidomide replicate most of the detectable birth defects associated with human thalidomide teratogenesis and demonstrate potentially novel deformities. Thalidomide exposed *M. domestica* embryos are defective in vascular, face, eye, and limb patterning. The lack of significant change in vasculature density may be caused by limitations of the assay rather than a lack of vascular malformations.

Unlike rabbits, affected embryos are very easy to generate, with a 60% penetrance of the mildly phenotype and a 12% penetrance of the severe phenotype. This is consistent with human case reports, which show that roughly 20% of thalidomide exposed infants were born with severe abnormalities (Lenz & Knapp, 1962). Many of the known human genetic pathways of thalidomide teratogenesis appear to be maintained in *M. domestica*. Thalidomide-treated *M. domestica* also show depleted VEGFA and KDR with increased expression of TGFβ.

This study also represents first full RNA sequencing project that has been performed on any thalidomide-treated organism. We have identified several candidate genes involved in thalidomide teratogenesis and the partial teratogenic resistance rodents have to the drug.

With a log fold change of 2.88, SHOX is one of the most significantly upregulated genes found in thalidomide-treated opossums. This homeobox gene is located on the X and Y chromosomes and is involved in bone growth and maturation, particularly in the limbs. Mutations in SHOX have been linked to Turner Syndrome, Langer mesomelic dysplasia, and Léri-Weill dyschondrosteosis (Clement-Jones et al., 2000; Rappold et al., 2002). Like thalidomide teratogenesis, all of these disorders are associated with greatly reduced limb size. People who suffer from Turner Syndrome and have been exposed to thalidomide during their development sometimes also display the same type of abnormally rotated joints, known as radial dysplasia. Most interestingly, neither this highly conserved gene nor any ortholog of it is present in rodents such as mice, rats and hamsters (Clement-Jones et al., 2000). The potential link between rodent resistance to thalidomide limb deformities and SHOX is worth further investigation.

Another set of genes identified by this study that have gone largely uninvestigated in the disruption of limb patterning by thalidomide are the later HOX genes, specifically HOXA11, HOXA13, and HOXD11-13. All of these genes are significantly upregulated in treated opossums. One of the major functions of this set of genes is to pattern the autopod and the posterior-most region of the embryo (Oberg, 2014). In line with this, multiple severely affected opossum embryos exhibit an overall reduction in size in their posterior region. Additionally, both opossums and humans that are severely affected by thalidomide tend have reduced digits, most commonly the first digit (Lenz & Knapp, 1962). The first digit

is believed to be patterned independently of the ZPA by overlapping HOXA13, GLI3R and TBX5 domains(Oberg, 2014). Establishment of the domain of the first digit is also dependent on the absence of HOXD10-12. Interestingly, thalidomide treatment upregulated HOXD12 expression with a log fold change of 2.590. This overexpression could contribute to the deletion of the first digit, but further analyses are needed to test this hypothesis.

This is also the first study to identify thalidomide-induced amniotic sac defects. We found amniotic sac constrictions both on and separate from the developing embryo after treatment with thalidomide. The embryo's full development inside some of these constrictions suggests that this was a fusion of the amniotic sac later in the pregnancy, rather than a patterning defect. Alternatively these could represent non-embryonated vesicles. While the cause of these defects is unclear, this could help understand some of the less regularly seen thalidomide defects such as the deletion of the distal portion of digits. Many of these deformities in humans closely resemble those caused by prenatal constrictions in anmniotic band syndrome, so much that the two disorders can be mistaken for each other(Goldfarb, Sathienkijkanchai, & Robin, 2009).

This study is also the first look and cellular proliferation and death in a susceptible mammal limb. This lack of change overall proliferation and death change is constant with studies in chick limb development(Therapontos et al., 2009). However the shift in proliferation to the margins of the limb bud is not present in chicken models and likely is a better representation of human thalidomide limb development.

In this study we demonstrate that *M. domestica* is distinctly well suited to study human thalidomide teratogenesis. Most thalidomide induced morphological and gene expression changes are conserved from *M. domestica* to humans. This study has also identified several candidate genes that are potentially involved in thalidomide limb patterning disruption. Now that the applicability of this model organism has been established, additional research is needed to further evaluate mechanism of thalidomide teratogenesis.

REFERENCES


Ando, Y., Fuse, E., & Figg, W. D. (2002). Thalidomide metabolism by the CYP2C subfamily. *Clinical Cancer Research, 8*(6), 1964-1973.

Azcoitia, V., Aracil, M., Martínez-A, C., & Torres, M. (2005). The homeodomain protein Meis1 is essential for definitive hematopoiesis and vascular patterning in the mouse embryo. *Developmental biology, 280*(2), 307-320.

Bolger, A. M., Lohse, M., & Usadel, B. (2014). Trimmomatic: a flexible trimmer for Illumina sequence data. *Bioinformatics*, btu170.

Calabrese, L., & Fleischer, A. B. (2000). Thalidomide: current and potential clinical applications. *The American journal of medicine, 108*(6), 487-495.

Clement-Jones, M., Schiller, S., Rao, E., Blaschke, R. J., Zuniga, A., Zeller, R., . . . Strachan, T. (2000). The short stature homeobox gene SHOX is involved in skeletal abnormalities in Turner syndrome. *Human molecular genetics, 9*(5), 695-702.

Crawford, A. (2013). Brazil's new generation of Thalidomide babies. *BBC Newsnight*.

Delahunt, C., & Lassen, L. (1964). Thalidomide syndrome in monkeys. *Science, 146*(3649), 1300-1305.

Dobin, A., Davis, C. A., Schlesinger, F., Drenkow, J., Zaleski, C., Jha, S., . . . Gingeras, T. R. (2013). STAR: ultrafast universal RNA-seq aligner. *Bioinformatics, 29*(1), 15-21.

Doroba, C. K., & Sears, K. E. (2010). The divergent development of the apical ectodermal ridge in the marsupial Monodelphis domestica. *The Anatomical Record, 293*(8), 1325-1332.

Dove, F. (2011). What's happened to Thalidomide babies? Retrieved from BBC.com website:

Du, W., Hattori, Y., Hashiguchi, A., Kondoh, K., Hozumi, N., Ikeda, Y., . . . Yamada, T. (2004). Tumor angiogenesis in the bone marrow of multiple myeloma patients and its alteration by thalidomide treatment. *Pathology international, 54*(5), 285-294.

Efstathiou, E., Troncoso, P., Wen, S., Do, K.-A., Pettaway, C. A., Pisters, L. L., . . . Logothetis, C. J. (2007). Initial modulation of the tumor microenvironment accounts for thalidomide activity in prostate cancer. *Clinical Cancer Research, 13*(4), 1224-1231.

Fischer, E. S., Böhm, K., Lydeard, J. R., Yang, H., Stadler, M. B., Cavadini, S., . . . Lingaraju, G. M. (2014). Structure of the DDB1-CRBN E3 ubiquitin ligase in complex with thalidomide. *Nature, 512*(7512), 49-53.

Gershbein, L. L. (1965). Effect of thalidomide on rat liver regeneration and diaphragm carbohydrate metabolism. *Biochemical pharmacology, 14*(5), 893-895.

Goldfarb, C. A., Sathienkijkanchai, A., & Robin, N. H. (2009). Amniotic constriction band: a multidisciplinary assessment of etiology and clinical presentation. *The Journal of Bone & Joint Surgery, 91*(Supplement 4), 68-75.

Hanken, J., & Wassersug, R. (1981). A new double-stain technique reveals the nature of the hard tissues. *Funct. Photog, 16*, 22-26.

Huang, D., Sherman, B., & Lempicki, R. (2008). Systematic and integrative analysis of large gene lists using DAVID bioinformatics resources. Nat Protocols 4: 44–57.

Ito, T., Ando, H., & Handa, H. (2011). Teratogenic effects of thalidomide: molecular mechanisms. *Cellular and Molecular Life Sciences, 68*(9), 1569-1579.

Ito, T., Ando, H., Suzuki, T., Ogura, T., Hotta, K., Imamura, Y., . . . Handa, H. (2010). Identification of a primary target of thalidomide teratogenicity. *Science, 327*(5971), 1345-1350.

Jacques, V., Czarnik, A. W., Judge, T. M., Van der Ploeg, L. H., & DeWitt, S. H. (2015). Differentiation of antiinflammatory and antitumorigenic properties of stabilized enantiomers of thalidomide analogs. *Proceedings of the National Academy of Sciences, 112*(12), E1471-E1479.

Kenyon, B. M., Browne, F., & D'amato, R. J. (1997). Effects of thalidomide and related metabolites in a mouse corneal model of neovascularization. *Experimental eye research, 64*(6), 971-978.

Keyte, A. L., & Smith, K. K. (2008). Opossum (monodelphis domestica): A marsupial development model. *Cold Spring Harbor Protocols, 2008*(10), pdb. emo104.

Knobloch, J., & Rüther, U. (2008). Shedding light on an old mystery: thalidomide suppresses survival pathways to induce limb defects. *Cell Cycle, 7*(9), 1121-1127.

Knobloch, J., Shaughnessy, J. D., & Rüther, U. (2007). Thalidomide induces limb deformities by perturbing the Bmp/Dkk1/Wnt signaling pathway. *The FASEB Journal, 21*(7), 1410-1421.

Kohlhase, J., Schubert, L., Liebers, M., Rauch, A., Becker, K., Mohammed, S., . . . Reardon, W. (2003). Mutations at the SALL4 locus on chromosome 20 result in a range of clinically overlapping phenotypes, including Okihiro syndrome, Holt-Oram syndrome, acro-renal-ocular syndrome, and patients previously reported to represent thalidomide embryopathy. *Journal of medical genetics, 40*(7), 473-478.

Komorowski, J., Jerczyńska, H., Siejka, A., Barańska, P., Ławnicka, H., Pawłowska, Z., & Stępień, H. (2006). Effect of thalidomide affecting VEGF secretion, cell migration, adhesion and capillary tube formation of human endothelial EA. hy 926 cells. *Life sciences, 78*(22), 2558-2563.

Lebrin, F., Srun, S., Raymond, K., Martin, S., van den Brink, S., Freitas, C., . . . Thomas, J.-L. (2010). Thalidomide stimulates vessel maturation and reduces epistaxis in individuals with hereditary hemorrhagic telangiectasia. *Nature medicine, 16*(4), 420-428.

Lenz, W., & Knapp, K. (1962). Thalidomide embryopathy. *Archives of Environmental Health: An International Journal, 5*(2), 14-19.

Loeys, B. L., Chen, J., Neptune, E. R., Judge, D. P., Podowski, M., Holm, T., . . . Sharifi, N. (2005). A syndrome of altered cardiovascular, craniofacial, neurocognitive and skeletal development caused by mutations in TGFBR1 or TGFBR2. *Nature genetics, 37*(3), 275-281.

Mercader, N., Leonardo, E., Azpiazu, N., Serrano, A., Morata, G., Martínez-A, C., & Torres, M. (1999). Conserved regulation of proximodistal limb axis development by Meis1/Hth. *Nature, 402*(6760), 425-429.

Mikkelsen, T. S., Wakefield, M. J., Aken, B., Amemiya, C. T., Chang, J. L., Duke, S., . . . Heger, A. (2007). Genome of the marsupial Monodelphis domestica reveals innovation in non-coding sequences. *Nature, 447*(7141), 167-177.

Miller, M. T., & Strömland, K. (1999). Teratogen update: thalidomide: a review, with a focus on ocular findings and new potential uses. *Teratology, 60*(5), 306-321.

Oberg, K. C. (2014). Review of the molecular development of the thumb: digit primera. *Clinical Orthopaedics and Related Research®, 472*(4), 1101-1105.

Parman, T., Wiley, M. J., & Wells, P. G. (1999). Free radical-mediated oxidative DNA damage in the mechanism of thalidomide teratogenicity. *Nature medicine, 5*(5), 582-585.

Qu, S., Niswender, K. D., Ji, Q., van der Meer, R., Keeney, D., Magnuson, M. A., & Wisdom, R. (1997). Polydactyly and ectopic ZPA formation in Alx-4 mutant mice. *Development, 124*(20), 3999-4008.

Rappold, G. A., Fukami, M., Niesler, B., Schiller, S., Zumkeller, W., Bettendorf, M., . . . Onigata, K. (2002). Deletions of the homeobox gene SHOX (short stature homeobox) are an important cause of growth failure in children with short stature. *The Journal of Clinical Endocrinology & Metabolism, 87*(3), 1402-1406.

Robinson, M. D., McCarthy, D. J., & Smyth, G. K. (2010). edgeR: a Bioconductor package for differential expression analysis of digital gene expression data. *Bioinformatics, 26*(1), 139-140.

Sato, T. N., Tozawa, Y., Deutsch, U., Wolburg-Buchholz, K., Fujiwara, Y., Gendron-Maguire, M., . . . Qin, Y. (1995). Distinct roles of the receptor tyrosine kinases Tie-1 and Tie-2 in blood vessel formation. *Nature, 376*(6535), 70-74.

Sekeres, M. A., & List, A. (2006). Immunomodulation in myelodysplastic syndromes. *Best Practice & Research Clinical Haematology, 19*(4), 757-767.

Smith, K. (2002). Monodelphis Staging Reference Series. 2015

Smithells, R., & Newman, C. (1992). Recognition of thalidomide defects. *Journal of medical genetics, 29*(10), 716.

Tamilarasan, K., Kolluru, G. K., Rajaram, M., Indhumathy, M., Saranya, R., & Chatterjee, S. (2006). Thalidomide attenuates nitric oxide mediated angiogenesis by blocking migration of endothelial cells. *BMC cell biology, 7*(1), 17.

Thakurta, A., Gandhi, A., Waldman, M., Bjorklund, C., Ning, Y., Mendy, D., . . . Schey, S. (2014). Absence of mutations in cereblon (CRBN) and DNA damage-binding protein 1 (DDB1) genes and significance for IMiD therapy. *Leukemia, 28*(5), 1129.

Therapontos, C., Erskine, L., Gardner, E. R., Figg, W. D., & Vargesson, N. (2009). Thalidomide induces limb defects by preventing angiogenic outgrowth during early limb formation. *Proceedings of the National Academy of Sciences, 106*(21), 8573-8578.

Theurl, M., Schgoer, W., Albrecht-Schgoer, K., Lener, D., Wolf, D., Wolf, M., . . . Fischer-Colbrie, R. (2015). Secretoneurin gene therapy improves hind limb and cardiac ischaemia in Apo E−/− mice without influencing systemic atherosclerosis. *Cardiovascular research, 105*(1), 96-106.

Tseng, S., Pak, G., Washenik, K., Pomeranz, M. K., & Shupack, J. L. (1996). Rediscovering thalidomide: a review of its mechanism of action, side effects, and potential uses. *Journal of the American Academy of Dermatology, 35*(6), 969-979.

Vargesson, N. (2009). Thalidomide-induced limb defects: resolving a 50-year-old puzzle. *Bioessays, 31*(12), 1327-1336.

Vargesson, N. (2013). Thalidomide embryopathy: an enigmatic challenge. *ISRN Developmental Biology, 2013*.

FIGURES AND TABLES

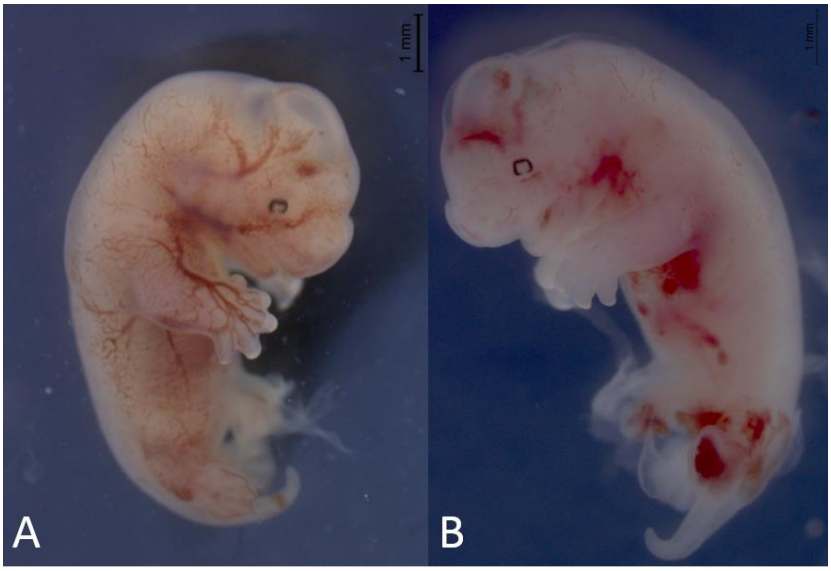



Figure 1: Embryos treated with thalidomide at stage 26 and photographed at stage 33. A: A healthy unaffected embryo. B: An embryo mildly affected by thalidomide treatment. Note the hemorrhaging below the on and around the hindlimb as well as above and below the forelimb

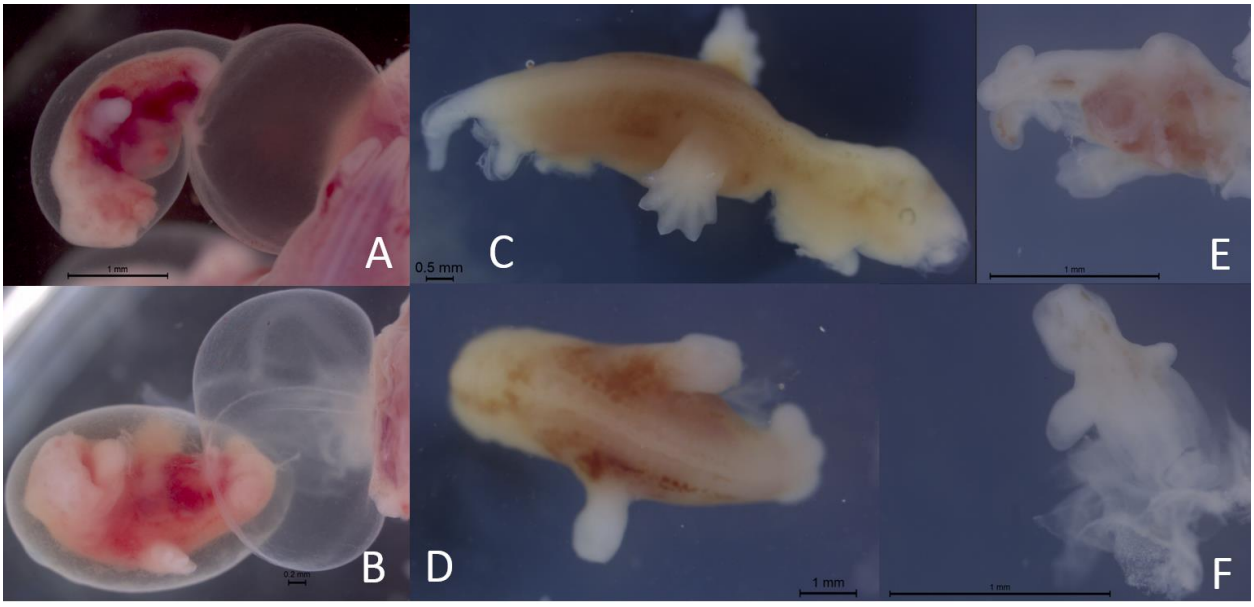



Figure 2: Severely deformed embryos treated with thalidomide at stage 26 and photographed at stage 33.
A: 1684-1 B: 699-1 C: 613-10 D: 627-1 E: 1684-2 F: 1684-3

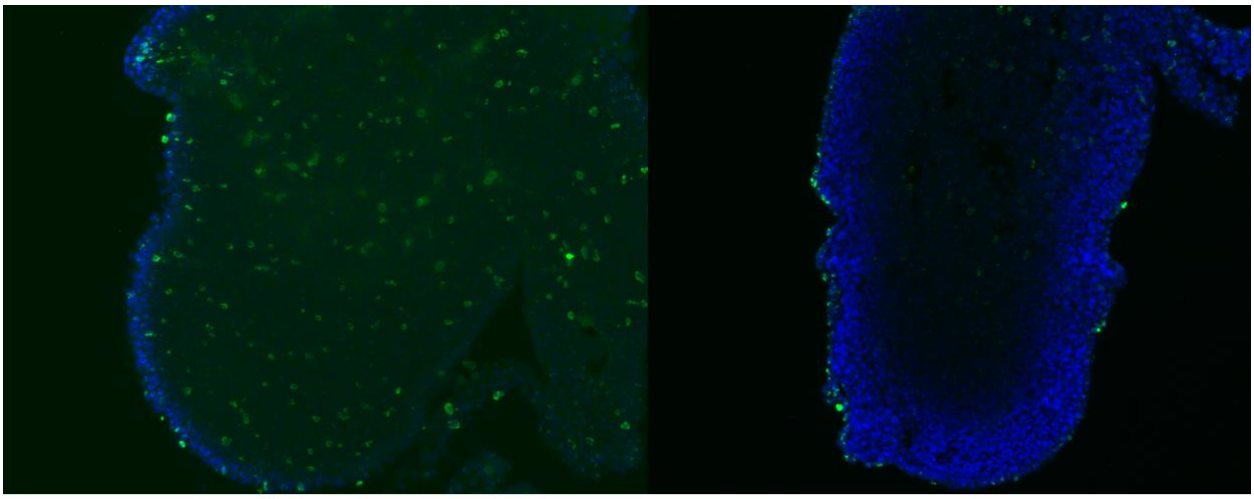


Figure 3: Two late stage 27 limb buds stained for proliferation against phospho-histone H3. The bud on the left has been treated with a DMSO loading control and the bud on the right has also been treated with thalidomide.

| *Go Term* | *% of unregulated genes represented* | *% of Go Term genes represented* | *P Value* | *Benjamini* |
|---|---|---|---|---|
| *Neuron Differentiation* | 7.99 | .9 | 9.3E-33 | 3.1E-29 |
| *Embryonic Morphogenesis* | 6.27 | .7 | 7.7E-30 | 1.3E-26 |
| *Skeletal System Development* | 5.61 | .6 | 6.3E-22 | 1.4E-19 |
| *Heart Development* | 4.16 | .5 | 1.3E-18 | 1.8E-16 |
| *Blood Vessel Development* | 3.70 | .3 | 3.4E-11 | 1.5E-9 |
| *Limb Development* | 2.18 | .2 | 3.9E-11 | 1.7E-9 |

Table 1: Up Regulated GO Terms

| *Gene* | *Log FC* | *P Value* | *FDR* |
|---|---|---|---|
| *ALX3* | 0.957 | 0.000566 | 0.002963 |
| *ALX4* | 1.295 | 1.47E-05 | 0.000123 |
| *APOE* | -2.558 | 6.56E-29 | 9.40E-27 |
| *Ang1* | 0.812 | 0.001155 | 0.005427 |
| *BMP6* | -3.604 | 2.82E-25 | 2.96E-23 |
| *BMPR2* | 1.311 | 3.48E-05 | 0.00026 |
| *DCC* | 2.891 | 6.88E-18 | 3.49E-16 |
| *GSR* | -0.789 | 1.93E-06 | 1.94E-05 |
| *HAND1* | -2.292 | 5.89E-21 | 4.08E-19 |
| *HOXA11* | 1.232 | 3.59E-07 | 4.26E-06 |
| *HOXA13* | 2.241 | 2.91E-12 | 7.84E-11 |
| *HOXA4* | 1.166 | 3.37E-05 | 0.000254 |
| *HOXA5* | 1.115 | 3.97E-07 | 4.67E-06 |
| *HOXD12* | 2.590 | 2.96E-21 | 2.17E-19 |
| *HOXD12* | 2.100 | 2.93E-14 | 9.85E-13 |
| *IRX2* | 0.708 | 0.000446 | 0.002435 |
| *IRX4* | 0.737 | 0.007207 | 0.025018 |
| *IRX5* | 0.816 | 0.009061 | 0.030189 |
| *KDR* | -0.758 | 3.86E-05 | 0.000284 |
| *MEIS1* | 0.818 | 1.12E-06 | 1.19E-05 |
| *MEIS2* | 0.642 | 6.26E-05 | 0.000436 |
| *POSTN* | 3.193 | 1.95E-28 | 2.68E-26 |
| *PTGES* | -4.586 | 4.33E-51 | 3.99E-48 |
| *RGCC* | -3.011 | 7.79E-46 | 3.86E-43 |
| *SHH* | 0.693 | 0.003237 | 0.013006 |
| *SHOX* | 2.884 | 1.46E-09 | 2.63E-08 |
| *SHOX2* | 2.334 | 3.34E-17 | 1.58E-15 |
| *SOX9* | 1.064 | 2.67E-09 | 4.54E-08 |
| *ST18* | 3.053 | 1.35E-15 | 5.28E-14 |
| *TBX4* | 1.913 | 4.17E-06 | 3.91E-05 |
| *TBX5* | 1.147 | 1.53E-05 | 0.000127 |
| *TEK* | -0.769 | 0.000881 | 0.004317 |
| *TGFBR2* | -1.084 | 2.63E-06 | 2.58E-05 |
| *VEGFA* | -1.945 | 6.04E-28 | 8.12E-26 |

Table 2: Selected differential expressed gene

| *Go Term* | *% of unregulated genes represented* | *% of Go Term genes represented* | *P Value* | *Benjamini* |
|---|---|---|---|---|
| *Organelle Membrane* | 15.53 | 1.1 | 1.3E-30 | 7.3E-28 |
| *Mitochondria* | 15.34 | 1.1 | 6.2E-30 | 1.7E-27 |
| *Endoplasmic Reticulum* | 8.20 | .7 | 5.1E-24 | 6.0E-22 |
| *Oxidation Reduction* | 9.28 | .7 | 1.3E-21 | 5.0E-18 |
| *Lipid Biosynthetic Process* | 4.90 | .4 | 1.8E-19 | 3.5E-16 |
| *Response to Wounding* | 4.41 | .3 | .022 | .31 |
| *Angiogenesis* | 1.45 | .1 | .049 | .5 |

Table 3: Down Regulated GO Terms